

Megakaryocyte-restricted MYH9 inactivation dramatically affects hemostasis while preserving platelet aggregation and secretion.

Catherine Léon, Anita Eckly, Béatrice Hechler, Boris Aleil, Monique Freund, Catherine Ravanat, Marie Jourdain, Christelle Nonne, Josiane Weber, Ralph Tiedt, et al.

▶ **To cite this version:**

Catherine Léon, Anita Eckly, Béatrice Hechler, Boris Aleil, Monique Freund, et al.. Megakaryocyte-restricted MYH9 inactivation dramatically affects hemostasis while preserving platelet aggregation and secretion.: Role of myosin IIA in hemostasis and thrombosis. Blood, 2007, 110 (9), pp.3183-91. 10.1182/blood-2007-03-080184 . inserm-00166437

HAL Id: inserm-00166437

https://inserm.hal.science/inserm-00166437

Submitted on 24 Jul 2008

HAL is a multi-disciplinary open access archive for the deposit and dissemination of scientific research documents, whether they are published or not. The documents may come from teaching and research institutions in France or abroad, or from public or private research centers.

L'archive ouverte pluridisciplinaire **HAL**, est destinée au dépôt et à la diffusion de documents scientifiques de niveau recherche, publiés ou non, émanant des établissements d'enseignement et de recherche français ou étrangers, des laboratoires publics ou privés.

HAL author manuscript

Blood , (2007) epub ahead of print

Megakaryocyte-restricted *MYH9* inactivation dramatically affects hemostasis while preserving platelet aggregation and secretion.

Catherine Léon[1], Anita Eckly[1], Béatrice Hechler[1], Boris Aleil[1], Monique Freund[1], Catherine Ravanat[1], Marie Jourdain[1], Christelle Nonne[1], Josiane Weber[1], Ralph Tiedt[2], Marie-Pierre Gratacap[3], Sonia Severin[3], Jean-Pierre Cazenave[1], François Lanza[1], Radek Skoda[2] and Christian Gachet[1]

[1] INSERM, U311, Strasbourg, France; EFS-Alsace, Strasbourg, France; Université Louis Pasteur, Strasbourg, UMR-S311, France.

[2] Department of Research, Experimental Hematology, University Hospital Basel, 4031 Basel, Switzerland.

[3] INSERM, U563, Centre de Physiopathologie de Toulouse, Département d'Oncogenèse et Signalisation dans les Cellules Hématopoïétiques, Toulouse, France; Université Toulouse III Paul Sabatier, Faculté de médecine Toulouse-Purpan, UMR-S563, Toulouse, France.

This study was supported by ARMESA (Association de Recherche et Développement en Médecine et Santé Publique) and Fondation de France (2007001964). C.L. and B.H. are supported by a "contrat d'interface" between EFS and INSERM.

Running head: Role of myosin IIA in hemostasis and thrombosis

Total text word count: 4886

Abstract word count: 199

Correspondence to:

C. LEON or Dr C. GACHET

INSERM U.311, Etablissement Français du Sang-Alsace (EFS-Alsace)

10, rue Spielmann, B.P. N° 36

67065 Strasbourg Cedex, France

Tel: (33) 388 21 25 25 Fax: (33) 388 21 25 21

e-mail: catherine.leon@efs-alsace.fr or christian.gachet@efs-alsace.fr

HAL author manuscript inserm-00166437, version 1

HAL author manuscript inserm-00166437, version 1

Scientific category: Hemostasis, Thrombosis, and Vascular Biology

Author's contribution statement

C. Leon designed and performed research, analyzed data and wrote the paper

A. Eckly performed and analyzed electron microscopy imaging

B. Hechler, M. Jourdain and C. Nonne performed and analysed in vitro thrombus formation and in vivo experimental thrombosis

C. Ravanat and B. Aleil designed and analysed flow cytometry experiments

M. Freund took care about the animals and performed animal experimentation

J. Weber constructed *MYH9* knockout mice

M-P. Gratacap and S. Severin performed and analysed phospholipids measurements

R. Tied and R. Skoda contributed with PF4-cre mice

J.-P. Cazenave discussed results

F. Lanza discussed results and wrote the paper

C. Gachet designed research, analysed the data and wrote the paper

HAL author manuscript inserm-00166437, version 1

Abstract

Mutations in the *MYH9* gene encoding the non-muscle myosin heavy chain-IIA result in bleeding disorders characterized by a macrothrombocytopenia. To understand the role of myosin in normal platelet functions and in pathology, we generated mice with disruption of *MYH9* in megakaryocytes. *MYH9*Δ mice displayed macrothrombocytopenia with a strong increase in bleeding time and absence of clot retraction. However, platelet aggregation and secretion in response to any agonist were near normal despite absence of initial platelet contraction. By contrast, integrin outside-in signaling was impaired, as observed by a decrease in integrin β3 phosphorylation and PtdIns(3,4)P_2 accumulation following stimulation. Upon adhesion on a fibrinogen-coated surface, *MYH9*Δ platelets were still able to extend lamellipodia but without stress fiber-like formation. As a consequence, thrombus growth and organization, investigated under flow by perfusing whole blood over collagen, were strongly impaired. Thrombus stability was also decreased *in vivo* in a model of $FeCl_3$-induced injury of carotid arteries. Overall, these results demonstrate that while myosin seems dispensable for aggregation and secretion in suspension, it plays a key role in platelet contractile phenomena and outside-in signaling. These roles of myosin in platelet functions, in addition to thrombocytopenia, account for the strong hemostatic defects observed in *MYH9*Δ mice.

HAL author manuscript inserm-00166437, version 1

Introduction

Important morphological changes occur in platelets during their activation at sites of vascular injury. The cells loose their resting discoid shape to become spheroid and contracted, emitting membrane blebs and longer extensions [1-4]. Once in contact with a surface, the spheroid platelets extend long filopodia and finally spread over it by emitting thin, sheet-like lamellipodia [1,2]. Myosin activation plays a central role in the cytoskeletal rearrangements underlying these changes in morphology. Myosin becomes activated after phosphorylation of the myosin regulatory light chain (RLC), which results from both calcium-regulated myosin light chain kinase activity and Rho kinase-regulated myosin phosphatase activity [5-8]. Activated myosin assembles into short filaments through the myosin heavy chain and interacts mainly with central actin filaments. Myosin has been proposed to participate in several platelet contractile functions such as platelet spheration, contraction and stress fiber formation, and fibrin clot retraction. Platelet spheration and contraction as observed in the aggregometer closely correlate with phosphorylation of the RLC [9,10] and are prevented when RLC phosphorylation is inhibited [6,7,9,10]. Myosin has also been shown to be associated with stress fiber-like structures in spreading adherent platelets [11]. In addition, myosin could play a role in platelet secretion as it is decreased by inhibition of myosin RLC phosphorylation [5,12-15]. Finally, a role of myosin in clot retraction has long been suspected in view of the necessity for a contractile force and was recently confirmed using a direct inhibitor of myosin activity [16].

Several of these platelet functions are altered in patients carrying mutations in the *MYH9* gene encoding the non-muscle myosin heavy chain IIA (NMHC-IIA) which is the only myosin heavy chain isoform present in platelets [17]. Mutations in this gene are responsible for the so-called *MYH9*-related disorders, which encompass several autosomal dominant diseases previously classified as May-Hegglin anomaly, Fechtner syndrome, Sebastian syndrome or Epstein syndrome [18-20]. Different mutations have been reported that in all cases result in

HAL author manuscript inserm-00166437, version 1

abnormal NMHC-IIA. All these patients share the triad of thrombocytopenia, large platelets and characteristic leukocyte inclusions (Döhle-like bodies) composed of ribosomes, endoplasmic reticulum and abnormal myosin aggregates [21,22]. Platelets from these patients fail to undergo shape change in the aggregometer in response to agonists but display normal aggregation [18,23-25]. While most patients are asymptomatic or have a mild bleeding tendency, a few suffer from significant bleeding, either spontaneously or during childbirth or surgical procedures [26]. Other manifestations may occur such as cataracts, sensorineural deafness or nephritis, which is consistent with the wide tissue expression of NMHC-IIA. Most of these other manifestations appear later during adulthood, probably because of the presence of other heavy chain isoforms in the tissues involved that compensate for the abnormal NMHC-IIA [20,27,28]. The molecular mechanisms leading to the platelet abnormalities are still subject to debate. Some studies suggested that mutations in *MYH9* led to a dominant negative effect, "poisoning" the wild-type myosin [21,29], others showed that the disease resulted from a haploinsufficiency [30] and a more recent study suggested haploinsufficiency in the megakaryocytic lineage associated with a dominant negative effect in granulocytes [31].

To explore the role of myosin and the effects of myosin deficiency on the hemostatic functions of platelets, we generated mice with disruption of *MYH9*. Since previous studies have shown early embryonic mortality in *MYH9*-/- mice [28,32] (and unpublished data), we used the loxP–Cre system to restrict the *MYH9* knock out to the megakaryocyte lineage. Mice carrying a floxed *MYH9* first exon were crossed with transgenic mice carrying cre-recombinase under the regulation of the platelet PF4 promoter [33]. Inactivation of *MYH9* in megakaryocytes resulted in a severe defect in platelet myosin expression with a phenotype resembling that of *MYH9*-related diseases, including thrombocytopenia, large and immature platelets and impaired platelet contractile activity. Our data show that whereas platelet aggregation and secretion responses were only moderately affected, myosin deficiency led to

dramatically disturbed primary hemostasis with severely prolonged tail bleeding times and a total absence of clot retraction. The platelet contractile shape change and outside-in signaling were affected, inhibiting thrombus growth *in vitro* under flow and *in vivo* following vessel wall injury.

HAL author manuscript inserm-00166437, version 1

HAL author manuscript inserm-00166437, version 1

Materials and Methods

Materials. Equine tendon collagen was from Nycomed (Germany) and human fibrinogen from Kabi (Sweden). BSA, Busulfan, thrombin and anti-NMHC-IIA antibody were from Sigma-Aldrich (France). Blebbistatin was from Calbiochem (VWR, France). Eptifibatid was from GlaxoSmithKline. Jon/A-PE antibody, FITC-labeled anti-fibrinogen antibody, anti-CD41/CD61-PE and anti-CD61 (β3 integrin) antibodies were from Emfret (Germany). Anti-β3 integrin [pY773] phosphospecific antibody was from Biosource International, Inc. (USA), anti-myosin RLC from Santa Cruz (USA) and the ECL kit from Amersham, Pharmacia Biotech (France). Phalloidin-Alexa Fluor 488 and goat anti rabbit-Alexa Fluor 488 antibody were from Molecular Probe (Invitrogen, France). Complete Protease Inhibitor Cocktail was from Roche Diagnostics (France).

Generation of megakaryocyte-restricted MYH9Δ mice. The contruction of floxed ES cells is detailed in supplementary figure 1. Floxed heterozygous mice (50% C57BL/6-50% 129sv) were crossed with transgenic mice selectively expressing cre-recombinase in the megakaryocyte lineage, under control of the BAC PF4 (platelet factor 4) promoter (100% C57BL/6)[33]. Mice expressing cre gene and heterozygous for the *MYH9* recombination were intercrossed to obtain littermate mice homozygous for the wild-type (WT) *MYH9* allele (+/+ mice) and homozygous for the recombined allele (*MYH9*Δ or -/- mice), or heterozygotes (+/- mice).

Bleeding time. Male and female mice (20-25g) were anesthetized by inhalation of isoflurane. The extremity of the mouse tail was cut transversally with a scalpel (3 mm) and immediately immersed in 0.9% isotonic saline at 37°C. The bleeding time was defined as the time required

HAL author manuscript inserm-00166437, version 1

for arrest of bleeding and when necessary bleeding was stopped manually at the 10 min time point to prevent death.

Clot retraction. Citrated PRP (adjusted to 3.10^5 platelets/µL, 300 µL) obtained by centrifugation of whole blood at 250g for 10 minutes was stimulated with thrombin (10 U/mL) in the presence of $CaCl_2$ (20 mM) and incubated at 37°C for up to 5 hours, together with 2 µL of erythrocytes to enhance the contrast of the clot.

Platelet survival. Platelet survival time was determined using a modified method adapted from Peng et al.[34] by *in vivo* biotinylation of platelets through intravenous injection of sulfo-NHS-Biotin (twice 2 mg/kg with 30 minutes interval, 5 mice of each genotype). Biotinylated platelets were counted daily for 4 days at 7 hour intervals. The percentage of biotinylated platelets was determined using flow cytometry by double labeling of whole blood with streptavidin-PE (100 µg/mL) and anti-CD41/CD61-PE.

Platelet activation studies. Blood was drawn from the abdominal aorta, platelets were washed and aggregation performed as described [35]. Platelet shape change was visualized by the decrease in light transmission in the absence of fibrinogen and in the presence of Eptifibatid (40 µg/mL) to prevent aggregation. Dense granule release was evaluated by the measure of serotonin secretion in platelets loaded with ^{3}H-5HT. In some cases, platelets were pretreated with blebbistatin (100 µM) for 30 minutes. Static adhesion assays were performed as previously described [36]. Briefly, coverslips were coated with fibrinogen (100 µg/mL), blocked with BSA (5 mg/mL) and washed. Platelet suspensions (2×10^4 platelets/µL) were stimulated with thrombin (1 U/mL), immediately plated onto the coverslips and incubated at 37°C for 45 min.

HAL author manuscript inserm-00166437, version 1

Immunofluorescence. Paraformaldehyde (2%) fixed platelets were permeabilized with 0.05% saponin in the presence of 0.2% bovine serum albumin, incubated with phalloidin-AF 488 or a primary antibody (anti NMHC-IIA, dilution 1/500) followed by a secondary antibody (goat anti rabbit-AF 488). The cells were observed under a confocal microscope (Leica TCS SP5, Leica Microsystems, France) with oil objectif (APO 100x, 1.30 NA). Surface area was quantified using Methamorph^{TM} software (Version 5; Universal Imaging Corporation, Downingtown, PA).

Flow cytometry. The activation state of the integrin αIIbβ3 was measured in washed platelets stimulated for 10 minutes with either collagen (100 µg/mL) or thrombin (1 U/mL) without stirring, followed by labeling with Jon/A-PE (1/20)[37]or FITC-labeled anti-fibrinogen antibody (1/20). The extent of integrin activation was determined for both antibodies by the geometric mean of the relative fluorescence intensity of the whole platelet population (in arbitrary units).

Western blotting. Frozen ground tissues lysates were prepared in 1% Triton X100 buffer. Platelet lysates were prepared by resuspending washed platelets (3 x 10^5/µL), activated or not by thrombin (1 U/mL) for various times, in SDS buffer (1% SDS final concentration). Proteins were separated by SDS-PAGE under reducing conditions, transferred to PVDF membranes and incubated with the primary antibody (antibody directed against NMHC-IIA, RLC, actin, β3 integrin or phosphorylated β3 integrin). Quantification was performed using the ImageQuant TL software v2003.03 (Amersham Biosciences). The amount of phosphorylated β3 integrin was normalized against total β3 integrin, and the NMHC-IIA was normalized against actin.

HAL author manuscript inserm-00166437, version 1

Lipid extraction and analysis. Platelets were labeled with 22 GBq/ml [^{32}P]orthophosphate during 45 min in a phosphate-free washing buffer (pH 6.5) [38] at 37°C, washed once and suspended at a final concentration of 5x10^5 platelets/µl (pH 7.38). After stimulation, reactions were stopped by addition of chloroform/methanol (1/1, v/v) containing 0.4 N HCl, and lipids were immediately extracted and quantified as described [38].

Electron microscopy. Platelets were fixed directly in the aggregometer cuvette with 2.5% glutaraldehyde in 0.1M cacodylate buffer, pH 7.2, containing 2% sucrose. Cells for transmission electron microscopy (TEM) were processed as described previously [35] and ultrathin sections were examined under a Philips CM120 Biotwin electron microscope (FEI, Eindhoven, The Netherlands) at 120 kV. Scanning electron microscopy (SEM) was performed as described elsewhere[37] under a Sirion scanning electron microscope (FEI) at 5 kV.

In vitro model of thrombosis on immobilized collagen under flow conditions. Platelet thrombus formation was studied as described previously[39]. Control wt mice were injected intraperitoneously with busulfan (30 mg/kg) 14 days before drawing blood so as to obtain a thrombocytopenia ranging from 1.10^5 to 3.10^5 platelets/µL. *MYH9*Δ mice were injected with vehicle (polyethylene-glycol). Hirudin anticoagulated whole blood was perfused through collagen-coated glass capillaries at a shear rate of 3,000 s^{-1}. For SEM analysis, the capillaries were rinsed with saline after blood perfusion for 2 minutes and the surface was fixed with 2.5% glutaraldehyde in 0.1 M cacodylate buffer (pH 7.2). The capillaries were sectioned longitudinally, treated and examined as described previously [40].

$FeCl_3$-induced carotid artery thrombosis. Carotid artery injury was performed by topical application of $FeCl_3$ for 2 minutes (Whatmann paper 1x0.5 mm soaked with 0.2 µL of 7.5% $FeCl_3$). The artery was then rinsed with saline and the thrombus growth was monitored for 20

HAL author manuscript inserm-00166437, version 1

minutes. DIOC6 (5 µL of a 100 µM solution/g of body weight) was injected into the jugular vein prior to injury to allow visualization of the thrombus surface. The carotid was placed under a fluorescent macroscope (Macrofluo^{TM}, Leica Microsystems, Rueil-Malmaison, France) for video recording of thrombosis[41]. Fluorescent images were acquired sequentially (1 image/s) using a CoolSNAP EZ camera (Ropper Scientific, Evry, France) controlled by Metaview software (Universal Imaging Corporation, Downingtown, PA). Quantification of embolism was performed using Metamorph^{TM} software. A region of interest was delineated downstream of the thrombus. Emboli surface was expressed as the total number of fluorescent pixels inside the region of interest, measured at each time.

Statistics. The results are expressed as mean±sem. The significance of the differences between genotypes was evaluated using Student t-test or Student Paired t-test, as mentioned.

HAL author manuscript inserm-00166437, version 1

Results

Generation of megakaryocyte-specific *MYH9*Δ mice

In order to generate a viable animal model with NMHC-IIA deficiency in the megakaryocytic lineage, we ablated exon 1 from the *MYH9* gene using a PF4-promoter driven Cre–loxP system. Exon 1 was excised *in vivo* (*MYH9*Δ) by crossing $MYH9^{Flx/Flx}$ mice with transgenic animals expressing cre-recombinase specifically in megakaryocytes under the control of the *PF4* promoter [33]. $MYH9^{Flx/wt}$; *PF4-cre* mice were intercrossed to produce platelet-specific NMHC-IIA deficient mice (Figure 1a and supplementary data), which were obtained in a mendelian ratio and were healthy, with no gross abnormality.

*MYH9*Δ mice exhibit severe NMHC-IIA deficiency

To determine the extent and tissue specificity of the NMHC-IIA deficiency, lysates from platelets and several tissues were analyzed by Western blotting. Normal myosin content was detected in kidney, lung, liver and spleen of *MYH9*Δ mice (Figure 1b). In contrast, a severe myosin deficiency was found in platelets where the residual myosin amounted to less than 3% of control platelets (Figure 1c, upper panel). The anti-myosin antibody being directed against the C-terminal part of the protein, this indicated that disruption of the first exon suppressed synthesis of most of the entire protein. A band of slightly lower molecular mass was also observed in *MYH9*Δ platelets only. This band could correspond to residual NMHC-IIA deleted from exon one since it is not observed in control platelets. The myosin regulatory light chain content was likewise considerably decreased in *MYH9*Δ platelets, probably due to its instability in the absence of NMHC-IIA (Figure 1c, lower panel) [42,43]. Platelet expression of the residual NMHC-IIA was visualized by immunofluorescence microscopy. As seen in

HAL author manuscript inserm-00166437, version 1

Figure 1d, the intensity of NMHC-IIA labeling was considerably reduced in all *MYH9*Δ platelets compared to control.

***MYH9*Δ mice display thrombocytopenia and altered platelet morphology**

Mice deficient in NMHC-IIA reproduced some of the characteristic features of *MYH9*-related diseases in humans. These mice exhibited thrombocytopenia with an average platelet count representing around 40% of wild-type (wt: 1028±63x10^3 platelets/µL, heterozygous: 890±41x10^3 platelets/µL, *MYH9*Δ: 336±28x10^3 platelets/µL) (Figure 2a). The decreased platelet count in heterozygote mice was not statistically different as compared to wt. These mice also presented an altered platelet morphology with a mean size around twice that of controls as determined by transmission electron microscopy performed on buffy coats (platelet area: 1.8±0.1 (n=215) *vs* 4.4±0.2 µm^2 (n=190) for control and *MYH9*Δ platelets respectively, $p<0.0001$, unpaired t-test) or by whole blood flow cytometry (FSC Geometric Mean of $\alpha_{IIb}\beta_3$-positive population: 15.1±1.3 for control mice *vs* 26.8±0.9 for *MYH9*Δ mice, n=5, $p<0.0001$ using unpaired t-test) (Figure 2b and 2c). Ultrastructural analysis of *MYH9*Δ washed platelets revealed some heterogeneity with a mixed population of normal discoid and more ovoid morphology, compared to the control platelets (Figure 2b and 2c). A large proportion of these platelets contained large amounts of rough endoplasmic reticulum (RER), typical of young or immature cells as observed both by electron microscopy (15.3% of *MYH9*Δ platelets vs. 0.5% of wt platelets, respectively) (Fig. 2d) and thiazole orange labeling (data not shown). Ultrastructure of platelets from heterozygous animals appeared normal (data not shown). There was no defect in expression of some major platelet glycoproteins ($\alpha_{IIb}\beta_3$, GPIbα, GPIbβ, GPV) as detected by flow cytometry (data not shown).

In vivo platelet half-life was similar in the two genotypes (survival time: 112.4±6.1 vs 101.6±4.6 hours for wt and *MYH9*Δ mice, respectively, n=5, $p>0.05$), suggesting that the

HAL author manuscript inserm-00166437, version 1

thrombocytopenia does not result from an accelerated clearance from the circulation and that the increased proportion of reticulated cells mostly reflects a defect in the formation of mature platelets.

_MYH9_Δ mice exhibit a strong increase in bleeding time and a total absence of clot retraction

*MYH9*Δ mice presented no evidence of spontaneous bleeding or hemorrhage. Tail bleeding times were performed to explore primary hemostasis functions following injury. Control wt mice had an average bleeding time of 78±16 s (Fig. 3a). An increased bleeding time up to 400 s was observed in some heterozygous mice but the average bleeding time was not significantly different from the wt (135±39 s). By contrast, all the *MYH9*Δ mice bled for more than 600 s. It is noteworthy that the bleeding was so important in these mice that they died by 20 minutes unless the wound was manually cauterized (data not shown). By comparison, busulfan-induced thrombocytopenia in wt mice (ranging from 0.3 to $0.6x10^6$ platelets/µL which is comparable to *MYH9*Δ mice) did not significantly affect the bleeding time (173± 24 s) (Figure 3a).

Clot retraction, a platelet-dependent contractile phenomenon important for thrombus consolidation, was then investigated. No retraction at all was observed in clots of myosin-deficient platelets 5 hour post-thrombin activation, while maximal retraction was observed for the wt platelets (Figure 3b). Heterozygous mice exhibited an intermediate phenotype, the retraction being delayed as compared to the wt (Figure 3b).

Thus an intrinsic platelet function defect accounts for this bleeding phenotype independently of the thrombocytopenia.

Platelet aggregation and secretion are barely affected by myosin deficiency

HAL author manuscript inserm-00166437, version 1

The defective hemostasis in *MYH9*Δ mice led us to investigate *in vitro* platelet aggregation in response to different concentrations of ADP, thrombin, collagen and U46619. The velocity and amplitude of aggregation were similar in *MYH9*Δ and control platelets except at the lowest concentration of thrombin (0.02 U/mL) and U46619 (0.5 and 0.1 µM) where a decreased aggregation was observed (Figure 4a). The transient decrease in light transmission which reflects platelet spheration (circled in the figure 4a) was absent in *MYH9*Δ cells, whatever the agonist. Release of [^{3}H]serotonin from dense granules was barely decreased in *MYH9*Δ platelets after stimulation with collagen or high concentrations of thrombin but more reduced after activation with U46619 or low concentrations of thrombin (Table 1). Altogether, there appears to be a minor impact if any of myosin-deficiency on platelet aggregation and secretion in suspension. In order to assess whether the residual myosin expression could play a part in the near normal aggregation and secretion observed, platelets were pretreated with blebbistatin (100 µM), an inhibitor of non-muscle myosin II activity [44,45]. Under these conditions, blebbistatin totally prevented initial platelet shape change in control platelets. However, no further inhibition of platelet aggregation or secretion was observed in *MYH9*Δ platelets (data not shown). Thus, these data show that myosin does not play a crucial role in these functions.

Myosin-deficient platelets display impaired contractile shape change and stress fibers formation

Platelet shape change was further investigated in the aggregometer following addition of 5 µM ADP in the absence of fibrinogen and in the presence of the integrin $\alpha_{IIb}\beta_3$ antagonist Eptifibatid to prevent platelet aggregation. As shown in Figure 4b, the shape change was almost abolished in *MYH9*Δ as compared to control platelets while platelets from heterozygous mice exhibited normal shape change (data not shown). Observation by SEM

HAL author manuscript inserm-00166437, version 1

revealed the presence of 92% discoid platelets with only a few or no membrane extensions whereas in the control 72% of the platelets underwent rounding and contraction (Figure 4b). Platelets from heterozygous animals behaved similarly to the control platelets (data not shown). Treatment of platelets with blebbistatin abolished rounding and contraction of control platelets by 96% and had no further significant effect on *MYH9*Δ platelets (data not shown).

Platelet spreading and stress fibers formation were then studied during adhesion of platelets to a fibrinogen-coated surface. When pre-stimulated with thrombin, both wt and *MYH9*Δ platelets were able to adhere to the surface and extend lamellipodia, as was revealed by phalloidin labeling of actin fibers (Figure 5a) and SEM after triton X100 permeabilization (Figure 5b). However, *MYH9*Δ platelets were unable to form stress fiber-like structures contrary to control platelets. Instead, long actin filaments were observed throughout the cytoplasm together with short filaments at the leading edge, and the final mean surface area was increased by 10% (n=736 and 670 platelets for control and *MYH9*Δ platelets, respectively, $p<0.0002$ using Student t-test).

Outside-in signaling is strongly impaired in myosin-deficient platelets

The absence of stress fibers formation on a fibrinogen matrix together with absent clot retraction prompted us to evaluate signaling through integrin αIIbβ3. Integrin activation was evaluated in control and *MYH9*Δ mice following activation by collagen (100 µg/mL) or thrombin (1 U/mL) in the absence of stirring. The level of activated integrin was measured by flow cytometry using an antibody directed against the activated form of the integrin (Jon/A PE antibody[37]) or against integrin-bound fibrinogen. In both cases, thrombin stimulation led to a significant decrease in αIIbβ3 activation that was not observed with collagen (Figure 6a).

Outside-in signaling was then evaluated by the phosphorylation of the integrin β3 during the course of thrombin-induced platelet aggregation. As shown by immunoblotting,

HAL author manuscript inserm-00166437, version 1

thrombin stimulation led to the phosphorylation of integrin β3 as early as 60 seconds following agonist addition in control platelets. By contrast, in *MYH9*Δ platelets, there was impairment in the phosphorylation of the integrin. By 3 minutes, the amount of integrin β3 phosphorylated in myosin-deficient platelets was decreased by 65% as compared to the wt platelets, indicating that myosin plays a role in integrin outside-in signaling (Figure 6b).

To further evaluate defective outside-in signaling, we measured the activity of PI 3-kinase. Particularly, the synthesis of a major part of one of its product, PtdIns(3,4)P_2, is indeed dependent upon the engagement of the integrin [46,47]. The levels of PtdIns(3,4)P_2 and PtdIns(3,4,5)P_3 were measured following platelet stimulation by thrombin or collagen. While the levels of PtdIns(3,4,5)P_2 were comparable between the two genotypes (not shown), PtdIns(3,4)P_2 accumulation was reduced by 70% in *MYH9*Δ platelets (Figure 6c), consistent with a defect in outside-in signaling.

Thrombus organization is impaired *in vitro* under flow conditions and *in vivo*

To evaluate the role of myosin in the process of thrombus formation, we first investigated thrombus growth *in vitro* in a whole blood perfusion assay over a fibrillar collagen matrix under arterial shear rate conditions (3,000 s^{-1}) [48]. Keeping in mind the decreased platelet count in *MYH9*Δ mice, wt mice were treated with busulfan to reach thrombocytopenia levels comparable to that of *MYH9*Δ mice (290±115x10^3 platelets/μL for busulfan-treated mice, and 220±103x10^3 platelets/μL for *MYH9*Δ mice). After 2 min perfusion, analysis of the flow chamber by SEM revealed that the structure of the thrombi was totally different between both genotypes. In the control condition, the compact aggregates formed were composed of contracted platelets tightly packed together. In contrast, aggregates of *MYH9*Δ blood contained only a few layers of platelets that did not have contracted bodies

HAL author manuscript inserm-00166437, version 1

and were rather flat with spread morphology, and were loosely packed as compared to the control cells (Figure 7a).

The capacity of *MYH9*Δ mice to develop a thrombus was then evaluated *in vivo* in a carotid artery thrombosis model where injury was induced by topical application of $FeCl_3$ and visualized by intravital microscopy[41] (Figure 7b and supplemental videos). Busulfan-treated wt mice were used as control. These mice exhibited a platelet count of $312\pm57x10^3$ platelets/µL (n=8) similar to platelet counts in *MYH9*Δ mice used in this experiment (317 ± 76 $x10^3$platelets/µL). In control mice, the thrombus was compact and occupied the whole injured surface as judged by the uniform intensity of fluorescence. By contrast, in *MYH9*Δ mice, the injured surface was not uniformly covered as observed by the lack of homogeneity of the fluorescence, indicating that platelets were not tightly packed and that the thrombus did not grow in height (Figure 7b and supplemental videos S1 and S2). In addition, large emboli were continuously detaching from the thrombus of *MYH9*Δ mice, suggesting instability of the thrombus (Figure 7c).

HAL author manuscript inserm-00166437, version 1

Discussion

In the present study, we addressed the question of the role of myosin and contractile activity in platelet functions. We established a mouse strain with megakaryocyte-restricted disruption of the *MYH9* gene, leading to severe NMHC-IIA deficiency in platelets amounting to less than 3% of the wt platelets. The reason for the presence of residual very low amounts myosin could be due to an incomplete excision of the *MYH9* exon 1 by the cre-recombinase in the megakaryocytes. Another possible explanation could be that the residual myosin reflects the long half-life of the NMHC-IIA synthesized before the time where the PF4 promoter becomes functional and promotes the expression of the Cre-recombinase. The appearance in the *MYH9*Δ platelets of a protein with a slightly lower molecular weight indicates that some synthesis from exon 1-deleted mRNA occurs. The presence of this protein in low amounts suggests that either the transcription or the traduction is not efficient, or that the truncated protein is unstable. In addition, the defect in NMHC-IIA expression led to a decrease in myosin RLC expression. This probably results from instability of the RLC in the absence of the heavy chain as already observed in Dictyostelium discoideum [43] and more recently in Drosophila melanogaster [42].

*MYH9*Δ mice presented a platelet phenotype closely resembling that of *MYH9*-related disorders in humans and consisting essentially of thrombocytopenia and large platelets, with an absence of agonist-induced platelet shape change [18]. However, due to its restriction to the megakaryocytic lineage, these mice lack additional defects observed in other tissues in *MYH9*-related diseases. The defect in protein expression in *MYH9*Δ platelets being more severe than the human defect, *MYH9*Δ mice could represent an interesting model to study some aspects of *MYH9*-related diseases in addition to the role of myosin in platelet functions.

HAL author manuscript inserm-00166437, version 1

The major observations were that *MYH9*Δ mice exhibited a considerable increase in the bleeding time and total absence of clot retraction. It is unlikely that the thrombocytopenia is the sole reason why *MYH9*Δ mice bled to death upon tail section. Indeed, busulfan-treated wt mice having thrombocytopenia in the same range as *MYH9*Δ mice displayed no such prolongation of the bleeding time. Moreover, in other severely thrombocytopenic mice such as cMpl, β1 tubulin or GPIbβ knockout mice [40,49,50] the bleeding tendency was likewise less pronounced. Hence our data suggest that altered platelet functions due to myosin deficiency are responsible for the defects.

The total absence of clot retraction may contribute to increase the bleeding time since impaired clot retraction has been shown to lead to rebleeding in several mouse models [51,52]. It is noteworthy that defective clot retraction has only been reported in a few *MYH9* patients[53] and one study mentioned normal clot retraction in a May-Hegglin subject who suffered from bleeding tendency [54]. One may speculate that some myosin activity are preserved in these patients, despite the presence of mutant forms of myosin IIA which are able to interact with the non mutated counterpart, thus "poisoning" the normal protein.

What makes the observation of increased bleeding time even more puzzling was that *in vitro* platelet aggregation and secretion were almost not altered in *MYH9*Δ mice. The very modest impact of myosin deficiency on secretion was unexpected since early observations that the cytoskeleton directs granule centralization in platelets had long led to the speculation that actomyosin should provide a contractile force facilitating the release of granule contents [55-57]. Furthermore, inhibitors of myosin light chain kinase or Rho-kinase have been shown to block phosphorylation of the myosin light chain, a prerequisite for myosin activation, and to inhibit the release reaction, suggesting that actomyosin contraction is required for granule secretion [5,12-15]. Our results indicate that myosin contraction, while facilitating the release

HAL author manuscript inserm-00166437, version 1

reaction following weak platelet stimulation, is in fact dispensable for platelet secretion when increasing agonist concentrations.

More unexpected, in view of the modest impact on platelet aggregation and secretion, was the alteration in thrombus formation both *in vitro* under high shear flow and *in vivo*. The disorganization of the thrombus in myosin-deficient mice is accompanied by an increase in emboli detaching from the thrombi. This effect on thrombus stability is most probably due to a decrease in aggregate stability under high shear forces that could result from both the absence of aggregate compaction and the defect in outside-in signaling. Indeed, aggregate compaction would be expected to allow the thrombus to resist shear forces and also to reduce the space between platelets, thus increasing local concentrations of released agonists. The capacity of platelets to remain in close contact to each other despite the shear forces rely on the engagement of integrins with their ligands, leading to signal transduction that reinforces the interactions between platelets. The αIIbβ3 integrin outside-in signaling resulting from fibrinogen binding leads to tyrosine phosphorylation of several proteins including the β3 subunit itself, activation of the phosphoinositide metabolism, further cytoskeleton reorganization, enhancement of platelet activation and improved stability of the aggregates [47,58]. Our results show that myosin plays a role in platelet integrin outside-in signaling as observed by a decrease in both PtdIns(3,4)P_2 accumulation and the β3 subunit phosphorylation. Phosphorylation of β3 allows direct interaction of the integrin with myosin. Platelets from DiYF mice, in which β3 cannot be tyrosine phosphorylated, exhibit like *MYH9*Δ platelets moderately impaired aggregation and unstable aggregate formation in response to low concentrations of thrombin, together with impaired clot retraction [52]. Thus actomyosin contractility may be important to control the extent of outside-in signaling, maybe through integrin clustering and focal adhesion maturation as is observed in other cells [59]. The way myosin IIA regulates focal adhesion through stress fibers formation may also contribute

HAL author manuscript inserm-00166437, version 1

to restrict lamellipodia extention in normal platelets following adhesion, similar to migrating cells where loss of NMHC-IIA-based contractility has been shown to relieve a restriction on protrusions extension [60].

In conclusion, inactivation of *MYH9* in the megakaryocytic lineage results in a severe deficiency in platelet myosin expression with a phenotype that partially resembles *MYH9*-related diseases in humans, including thrombocytopenia and large platelets. In one hand, our results highlight the important role of myosin IIA in outside-in signaling, clot retraction and thrombus formation and organization which, in addition to thrombocytopenia, account for the deficient hemostasis observed in *MYH9*Δ mice. On the other hand, myosin plays no major role in platelet aggregation and secretion in suspension. Homozygous gene inactivation obtained in *MYH9*Δ mice differ from the genetic defects resulting from mutations in one *MYH9* allele in patients with *MYH9*-related disorders. In these patients, expression of abnormal myosin is responsible for the pathology. Although this is probably the reason why patients have a less severe hemorrhagic syndrome than mice, the mechanisms described here nevertheless may explain part of the defects of hemostasis observed in the patients.

Acknowledgments

We thank Bernard Payrastre for critical reading of the manuscript. We thank Dominique Cassel, Patricia Laeuffer, Stéphanie Magnenat, Fabienne Proamer, Jean-Yves Rinckel, and Catherine Meyer for expert technical assistance, and J. N. Mulvihill for reviewing the English of the manuscript.

HAL author manuscript inserm-00166437, version 1

References

1. Barkalow KL, Falet H, Hartwig JH. Dynamics of the platelet cytoskeleton. In: Gresele P, Page C, Fuster V, Vermylen J, eds. Platelets in thrombotic and non-thrombotic disorders. Cambridge: Cambridge University Press; 2002:93-103.
2. Gear ARL, Polanowska-Grabowska Rk. The platelet shape change. In: Gresele P, Page C, Fuster V, Vermylen J, eds. Platelets in thrombotic and non-thrombotic disorders. Cambridge: Cambridge University Press; 2002:319-337.
3. Fox JE. The platelet cytoskeleton. Thromb Haemost. 1993;70:884-893.
4. Fox JE. Cytoskeletal proteins and platelet signaling. Thromb Haemost. 2001;86:198-213.
5. Suzuki Y, Yamamoto M, Wada H, et al. Agonist-induced regulation of myosin phosphatase activity in human platelets through activation of Rho-kinase. Blood. 1999;93:3408-3417.
6. Paul BZ, Daniel JL, Kunapuli SP. Platelet shape change is mediated by both calcium-dependent and -independent signaling pathways. Role of p160 Rho-associated coiled-coil-containing protein kinase in platelet shape change. J Biol Chem. 1999;274:28293-28300.
7. Bauer M, Retzer M, Wilde JI, et al. Dichotomous regulation of myosin phosphorylation and shape change by Rho-kinase and calcium in intact human platelets. Blood. 1999;94:1665-1672.
8. Klages B, Brandt U, Simon MI, Schultz G, Offermanns S. Activation of G12/G13 results in shape change and Rho/Rho-kinase-mediated myosin light chain phosphorylation in mouse platelets. J Cell Biol. 1999;144:745-754.
9. Daniel JL, Molish IR, Rigmaiden M, Stewart G. Evidence for a role of myosin phosphorylation in the initiation of the platelet shape change response. J Biol Chem. 1984;259:9826-9831.
10. Nachmias VT, Kavaler J, Jacubowitz S. Reversible association of myosin with the platelet cytoskeleton. Nature. 1985;313:70-72.
11. Tanaka K, Itoh K. Reorganization of stress fiber-like structures in spreading platelets during surface activation. J Struct Biol. 1998;124:13-41.
12. Lokeshwar VB, Bourguignon LY. The involvement of Ca2+ and myosin light chain kinase in collagen-induced platelet activation. Cell Biol Int Rep. 1992;16:883-897.
13. Nishikawa M, Tanaka T, Hidaka H. Ca2+-calmodulin-dependent phosphorylation and platelet secretion. Nature. 1980;287:863-865.
14. Saitoh M, Naka M, Hidaka H. The modulatory role of myosin light chain phosphorylation in human platelet activation. Biochem Biophys Res Commun. 1986;140:280-287.
15. Watanabe Y, Ito M, Kataoka Y, et al. Protein kinase C-catalyzed phosphorylation of an inhibitory phosphoprotein of myosin phosphatase is involved in human platelet secretion. Blood. 2001;97:3798-3805.
16. Suzuki-Inoue K, Hughes CE, Inoue O, et al. Involvement of Src kinases and PLCgamma2 in clot retraction. Thromb Res. 2006.
17. Berg JS, Powell BC, Cheney RE. A millennial myosin census. Mol Biol Cell. 2001;12:780-794.
18. Noris P, Spedini P, Belletti S, Magrini U, Balduini CL. Thrombocytopenia, giant platelets, and leukocyte inclusion bodies (May-Hegglin anomaly): clinical and laboratory findings. Am J Med. 1998;104:355-360.
19. Seri M, Cusano R, Gangarossa S, et al. Mutations in MYH9 result in the May-Hegglin anomaly, and Fechtner and Sebastian syndromes. The May-Heggllin/Fechtner Syndrome Consortium. Nat Genet. 2000;26:103-105.

HAL author manuscript inserm-00166437, version 1

20. Heath KE, Campos-Barros A, Toren A, et al. Nonmuscle myosin heavy chain IIA mutations define a spectrum of autosomal dominant macrothrombocytopenias: May-Hegglin anomaly and Fechtner, Sebastian, Epstein, and Alport-like syndromes. Am J Hum Genet. 2001;69:1033-1045.
21. Kunishima S, Matsushita T, Kojima T, et al. Immunofluorescence analysis of neutrophil nonmuscle myosin heavy chain-A in MYH9 disorders: association of subcellular localization with MYH9 mutations. Lab Invest. 2003;83:115-122.
22. Pujol-Moix N, Kelley MJ, Hernandez A, Muniz-Diaz E, Espanol I. Ultrastructural analysis of granulocyte inclusions in genetically confirmed MYH9-related disorders. Haematologica. 2004;89:330-337.
23. Canobbio I, Noris P, Pecci A, Balduini A, Balduini CL, Torti M. Altered cytoskeleton organization in platelets from patients with MYH9-related disease. J Thromb Haemost. 2005;3:1026-1035.
24. Heynen MJ, Blockmans D, Verwilghen RL, Vermylen J. Congenital macrothrombocytopenia, leucocyte inclusions, deafness and proteinuria: functional and electron microscopic observations on platelets and megakaryocytes. Br J Haematol. 1988;70:441-448.
25. Lusher JM, Barnhart MI. Congenital disorders affecting platelets. Semin Thromb Hemost. 1977;4:123-186.
26. Jantunen E. Inherited giant platelet disorders. Eur J Haematol. 1994;53:191-196.
27. D'Apolito M, Guarnieri V, Boncristiano M, Zelante L, Savoia A. Cloning of the murine non-muscle myosin heavy chain IIA gene ortholog of human MYH9 responsible for May-Hegglin, Sebastian, Fechtner, and Epstein syndromes. Gene. 2002;286:215-222.
28. Matsushita T, Hayashi H, Kunishima S, et al. Targeted disruption of mouse ortholog of the human MYH9 responsible for macrothrombocytopenia with different organ involvement: hematological, nephrological, and otological studies of heterozygous KO mice. Biochem Biophys Res Commun. 2004;325:1163-1171.
29. Franke JD, Dong F, Rickoll WL, Kelley MJ, Kiehart DP. Rod mutations associated with MYH9-related disorders disrupt nonmuscle myosin-IIA assembly. Blood. 2005;105:161-169.
30. Deutsch S, Rideau A, Bochaton-Piallat ML, et al. Asp1424Asn MYH9 mutation results in an unstable protein responsible for the phenotypes in May-Hegglin anomaly/Fechtner syndrome. Blood. 2003;102:529-534.
31. Pecci A, Noris P, Invernizzi R, et al. Immunocytochemistry for the heavy chain of the non-muscle myosin IIA as a diagnostic tool for MYH9-related disorders. Br J Haematol. 2002;117:164-167.
32. Conti MA, Even-Ram S, Liu C, Yamada KM, Adelstein RS. Defects in cell adhesion and the visceral endoderm following ablation of nonmuscle myosin heavy chain II-A in mice. J Biol Chem. 2004;279:41263-41266.
33. Tiedt R, Schomber T, Hao-Shen H, Skoda RC. Pf4-Cre transgenic mice allow generating lineage-restricted gene knockouts for studying megakaryocyte and platelet function in vivo. Blood. 2006.
34. Peng J, Friese P, Heilmann E, George JN, Burstein SA, Dale GL. Aged platelets have an impaired response to thrombin as quantitated by P-selectin expression. Blood. 1994;83:161-166.
35. Leon C, Hechler B, Freund M, et al. Defective platelet aggregation and increased resistance to thrombosis in purinergic P2Y(1) receptor-null mice. J Clin Invest. 1999;104:1731-1737.
36. McCarty OJ, Larson MK, Auger JM, et al. Rac1 is essential for platelet lamellipodia formation and aggregate stability under flow. J Biol Chem. 2005;280:39474-39484.

HAL author manuscript inserm-00166437, version 1

37. Kauffenstein G, Bergmeier W, Eckly A, et al. The P2Y(12) receptor induces platelet aggregation through weak activation of the alpha(IIb)beta(3) integrin--a phosphoinositide 3-kinase-dependent mechanism. FEBS Lett. 2001;505:281-290.
38. Payrastre B. Phosphoinositides: lipid kinases and phosphatases. Methods Mol Biol. 2004;273:201-212.
39. Strassel C, Nonne C, Eckly A, et al. Decreased thrombotic tendency in mouse models of the Bernard-Soulier syndrome. Arterioscler Thromb Vasc Biol. 2007;27:241-247.
40. Strassel C, Nonne C, Eckly A, et al. Decreased thrombotic tendency in mouse models of the Bernard-Soulier syndrome. Arterioscler Thromb Vasc Biol. 2006;in press.
41. Gross S, Tilly P, Hentsch D, Vonesch JL, Fabre JE. Vascular wall-produced prostaglandin E2 exacerbates arterial thrombosis and atherothrombosis through platelet EP3 receptors. J Exp Med. 2007;204:311-320.
42. Franke JD, Boury AL, Gerald NJ, Kiehart DP. Native nonmuscle myosin II stability and light chain binding in Drosophila melanogaster. Cell Motil Cytoskeleton. 2006;63:604-622.
43. Knecht DA, Loomis WF. Developmental consequences of the lack of myosin heavy chain in Dictyostelium discoideum. Dev Biol. 1988;128:178-184.
44. Limouze J, Straight AF, Mitchison T, Sellers JR. Specificity of blebbistatin, an inhibitor of myosin II. J Muscle Res Cell Motil. 2004;25:337-341.
45. Straight AF, Cheung A, Limouze J, et al. Dissecting temporal and spatial control of cytokinesis with a myosin II Inhibitor. Science. 2003;299:1743-1747.
46. Guinebault C, Payrastre B, Racaud-Sultan C, et al. Integrin-dependent translocation of phosphoinositide 3-kinase to the cytoskeleton of thrombin-activated platelets involves specific interactions of p85 alpha with actin filaments and focal adhesion kinase. J Cell Biol. 1995;129:831-842.
47. Payrastre B, Missy K, Trumel C, Bodin S, Plantavid M, Chap H. The integrin alpha IIb/beta 3 in human platelet signal transduction. Biochem Pharmacol. 2000;60:1069-1074.
48. Nonne C, Lenain N, Hechler B, et al. Importance of platelet phospholipase Cgamma2 signaling in arterial thrombosis as a function of lesion severity. Arterioscler Thromb Vasc Biol. 2005;25:1293-1298.
49. Bunting S, Widmer R, Lipari T, et al. Normal platelets and megakaryocytes are produced in vivo in the absence of thrombopoietin. Blood. 1997;90:3423-3429.
50. Schwer HD, Lecine P, Tiwari S, Italiano JE, Jr., Hartwig JH, Shivdasani RA. A lineage-restricted and divergent beta-tubulin isoform is essential for the biogenesis, structure and function of blood platelets. Curr Biol. 2001;11:579-586.
51. Goschnick MW, Lau LM, Wee JL, et al. Impaired "outside-in" integrin alphaIIbbeta3 signaling and thrombus stability in TSSC6-deficient mice. Blood. 2006;108:1911-1918.
52. Law DA, DeGuzman FR, Heiser P, Ministri-Madrid K, Killeen N, Phillips DR. Integrin cytoplasmic tyrosine motif is required for outside-in alphaIIbbeta3 signalling and platelet function. Nature. 1999;401:808-811.
53. Godwin HA, Ginsburg AD. May-Hegglin anomaly: a defect in megakaryocyte fragmentation? Br J Haematol. 1974;26:117-128.
54. Volpe E, Cuccurullo L, Valente A, Jori GP, Buonanno G. The May-Hegglin anomaly. Further studies on leukocyte inclusions and platelet ultrastructure. Acta Haematol. 1974;52:238-247.
55. Painter RG, Ginsberg MH. Centripetal myosin redistribution in thrombin-stimulated platelets. Relationship to platelet Factor 4 secretion. Exp Cell Res. 1984;155:198-212.
56. Gerrard JM, Israels SJ, Friesen LL. Protein phosphorylation and platelet secretion. Nouv Rev Fr Hematol. 1985;27:267-273.

HAL author manuscript inserm-00166437, version 1

57. White JG, Gerrard JM. Recent advances in platelet structural physiology. Suppl Thromb Haemost. 1978;63:49-60.
58. Phillips DR, Prasad KS, Manganello J, Bao M, Nannizzi-Alaimo L. Integrin tyrosine phosphorylation in platelet signaling. Curr Opin Cell Biol. 2001;13:546-554.
59. Chrzanowska-Wodnicka M, Burridge K. Rho-stimulated contractility drives the formation of stress fibers and focal adhesions. J Cell Biol. 1996;133:1403-1415.
60. Sandquist JC, Swenson KI, Demali KA, Burridge K, Means AR. Rho kinase differentially regulates phosphorylation of nonmuscle myosin II isoforms A and B during cell rounding and migration. J Biol Chem. 2006;281:35873-35883.

HAL author manuscript inserm-00166437, version 1

Table 1: Percentage 5 HT secretion in wt and *MYH9*Δ mice

Agonists	control (wt)	*MYH9*Δ
Thrombin (1 U/mL)	100	84.0±10
Thrombin (0.03 U/mL)	10.7±3.8	1.2±0.91
Collagen (100 µg/mL)	100	93.0±2.5
Collagen (5 µg/mL)	79.7±1.3	62.3±3.8$^{\square}$
U46619 (1 µM)	24.0±0.6	2.7±1.3†

Mean±sem of 3 independent experiments, $^{\square}p<0.05$, † $p<0.01$, Student Paired t-test.

HAL author manuscript inserm-00166437, version 1

Figure Legends

Figure 1. Generation of a platelet-specific *MYH9* knock-down mouse strain exhibiting myosin deficiency. (a) ES cells recombined with the floxed allele were injected into blastocysts to produce chimeric floxed mice (i). Deletion of the *MYH9* exon1 (*MYH9*Δ*)* was obtained by exposing the floxed allele to *in vivo* cre-recombinase expression (ii). (b) Western blot showing NMCH-IIA expression in several tissues from *MYH9*Δ mice (-/-) and control mice (+/+). An identical amount of protein lysate for control or *MYH9*Δ platelets was loaded in each lane, as shown by the similar levels of actin. (c) Upper panel: Western blot performed with increasing amounts of lysate from control (+/+) and *MYH9*Δ (-/-) platelets (numbers indicate the amount in µg of protein loaded on the gel), showing the residual myosin expressed in platelets (large grey arrow) and exon 1-deleted myosin (small black arrow). Lower panel: Western blot showing the regulatory light chain (RLC) expression in control and *MYH9*Δ platelets. (d) The entire population of platelets displayed decreased myosin content in *MYH9*Δ, as revealed by confocal immunofluorescence microscopy (one image representative of 3 independent mice). Bars 2 µm.

Figure 2. Platelet counts and ultrastructure. (a) *MYH9*Δ mice exhibited thrombocytopenia. The mean is represented in the figure (n=17-18). (b-c) Heterogeneity in platelet size as observed both by transmission electron microscopy (left panels) and by flow cytometry (right panels, showing representative dot plots of whole blood: FSC, forward scatter; SSC, side scatter; $\alpha_{IIb}\beta_3$-positive platelets are visualized by red dots). Control (b) and *MYH9*Δ (c) mouse platelets, bars 2 µm. (d) Higher magnification of a *MYH9*Δ platelet showing the highly developed rough endoplasmic reticulum. Bar 2 µm.

HAL author manuscript inserm-00166437, version 1

Figure 3. **Bleeding time and clot retraction.** (a) *MYH9*Δ mice had an increased bleeding time. Points indicate the time required for the arrest of bleeding and when necessary bleeding was stopped manually after 10 min. Control wt mice, grey circles, n=13; heterozygous mice, open squares, n=14; *MYH9*Δ mice, black triangles, n=21; wt mice treated with busulfan to achieve thrombocytopenia comparable to that of *MYH9*Δ mice, grey triangles, n=20. (b) Clot retraction was totally abolished in PRP from *MYH9*Δ mice, while it was delayed in heterozygous mice. The photograph corresponds to a 2 and 5-hour reaction in cPRP adjusted to 3.10^5 platelets/µL and treated with 10 U/mL thrombin and is representative of 3 experiments.

Figure 4. Platelet aggregation is preserved in *MYH9*Δ mice despite absence of initial shape change. (a) Platelet aggregation in response to ADP, thrombin, collagen and U46619 were barely impaired in *MYH9*Δ mice (numbers correspond to the concentration of agonist). The initial platelet contraction responsible for a transient decrease in light transmission (circled) was absent in *MYH9*Δ platelets. Tracings are representative of at least 3 experiments. (b) Shape change was evaluated in the aggregometer after stimulation of washed platelets with 5 µM ADP in the absence of fibrinogen and the presence of Eptifibatid. Shape change was visualized by scanning electron microscopy and by the decrease in light transmission (inset), representative of 3 independent experiments. Bars 2 µm.

Figure 5. Defective stress-fiber formation during spreading of *MYH9*Δ platelets. Platelets were pretreated with thrombin (1 U/mL) and allowed to adhere for 45 min to fibrinogen-coated coverslips. Actin filaments were visualized (a) by confocal fluorescence microscopy

HAL author manuscript inserm-00166437, version 1

after phalloidin-AF 488 labeling (bars 25 µm, inset 7.5 µm) and (b) by SEM after Triton X100 permeabilization (bars 2 µm). Representative of 3 experiments.

Figure 6. αIIbβ3 integrin activation and outside-in signaling in *MYH9*Δ platelets. (a) Flow cytometry experiments showing integrin $\alpha_{IIb}\beta_3$ activation as revealed by Jon/A-PE (left panel) or fibrinogen (right panel) labeling following platelet activation by thrombin (thr, 1U/mL) or collagen (coll, 100 µg/mL) in the absence of agitation. The amount of activated integrin is indicated by the geometric mean of the relative fluorescence intensity, in arbitrary units. Grey and black bars represent control and *MYH9*Δ platelets, respectively; mean ± standard error mean (sem), n=3 experiments. (b) Western blots showing phosphorylation of integrin β3 at Y773 (upper panel) during stimulation of platelets suspension by thrombin (1U/mL) for up to 3 min in the aggregometer. Identical protein loading was checked by reblotting with an anti-β3 antibody (lower panel). Blots are representative of 2 experiments. (c) PtdIns(3,4)P_2 synthesis following thrombin (1 U/mL) or collagen (10 µg/mL) stimulation upon 2 minutes. Values have been normalized against total polyphosphoinositides and the results are presented as fold increase compared to non stimulated platelets (±sem, n=3 independent experiments).

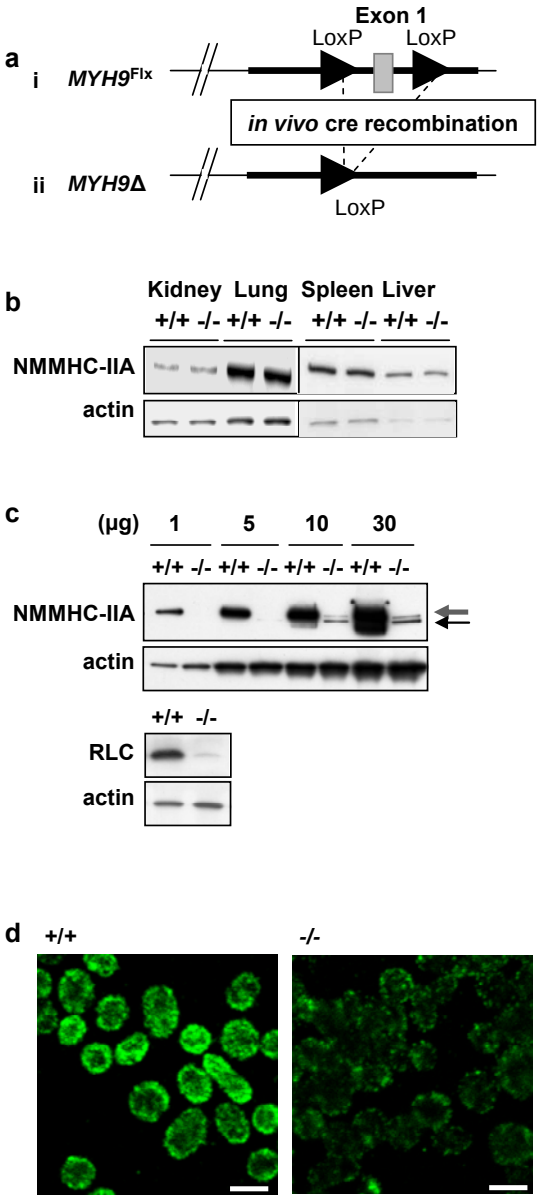
Figure 7. Defective thrombus formation *in vitro* and *in vivo*. (a) Whole blood from busulfan-treated wt mice (+/+) or *MYH9*Δ mice (-/-) was anticoagulated with hirudin (100 U/mL) and perfused through collagen-coated glass capillaries at a shear rate of 3000 s^{-1}. Scanning electron microscopy imaging was performed after 2 min perfusion and images are representative of 3 experiments. Bars 20 µm (upper panels) and 5 µm (lower panels). (b) $FeCl_3$-induced injury was performed in the carotid of busulfan-treated wt mice (+/+) or *MYH9*Δ mice (-/-) and the thrombus growth was video recorded. Images are representative of

8 mice, at time 600 s following injury (original magnification X45). (c) Time courses of the embolus surface area measured by the fluorescence passing through the region of interest (white square in the insert), downstream of the thrombus. Busulfan-treated mice (grey curve) and *MYH9*Δ mice (black curve); n=8, $p<0.0001$ (Student Paired t-test).

HAL author manuscript inserm-00166437, version 1

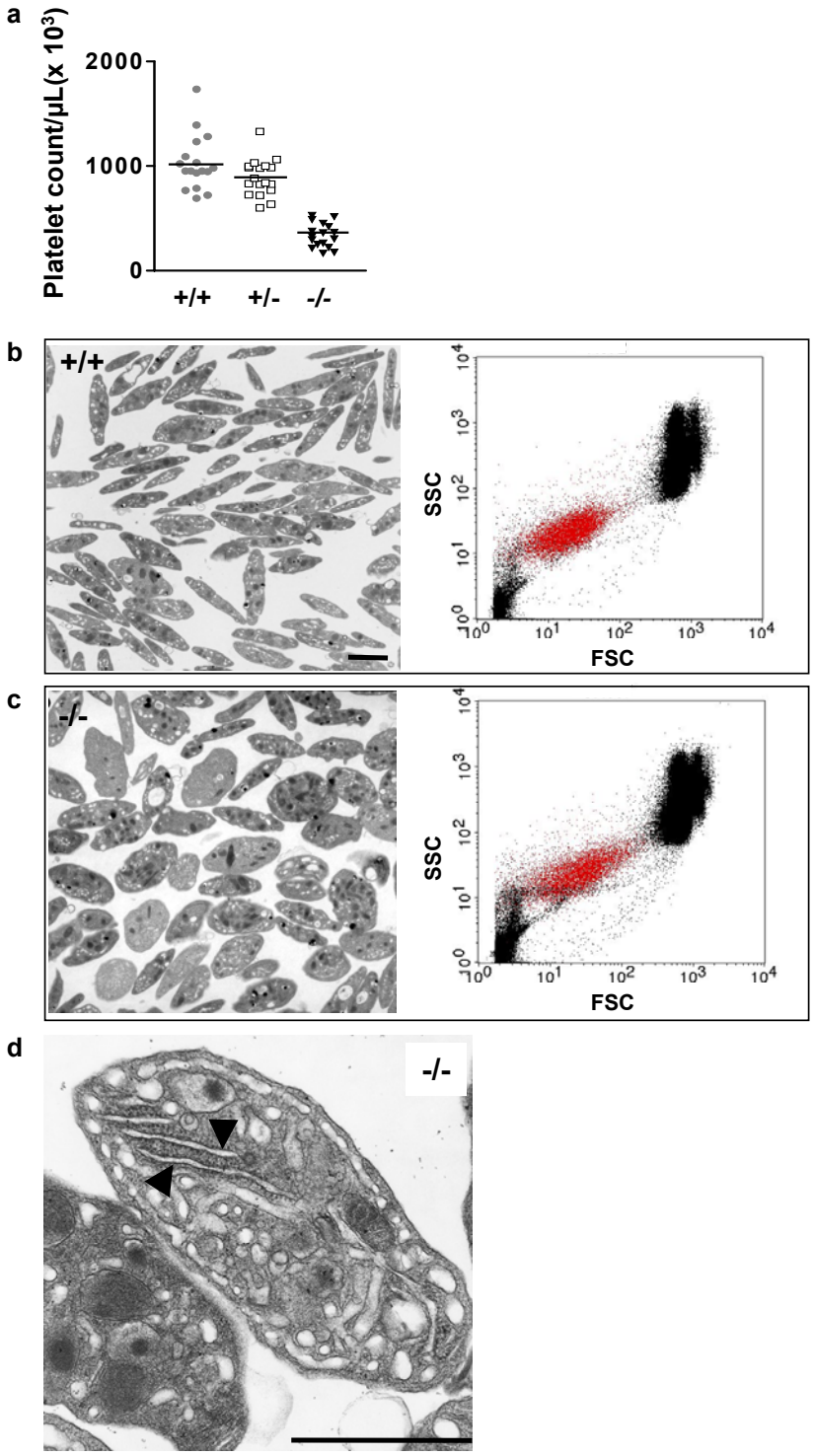
HAL author manuscript inserm-00166437, version 1

Figure 1



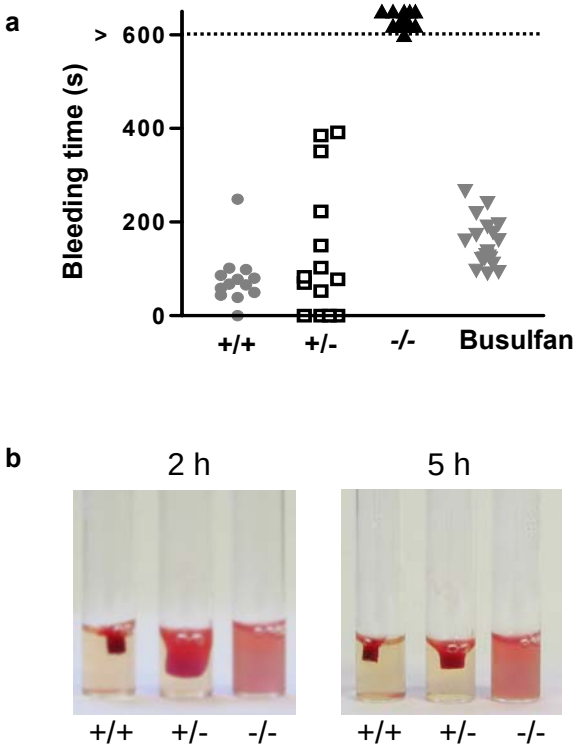
HAL author manuscript inserm-00166437, version 1

Figure 2



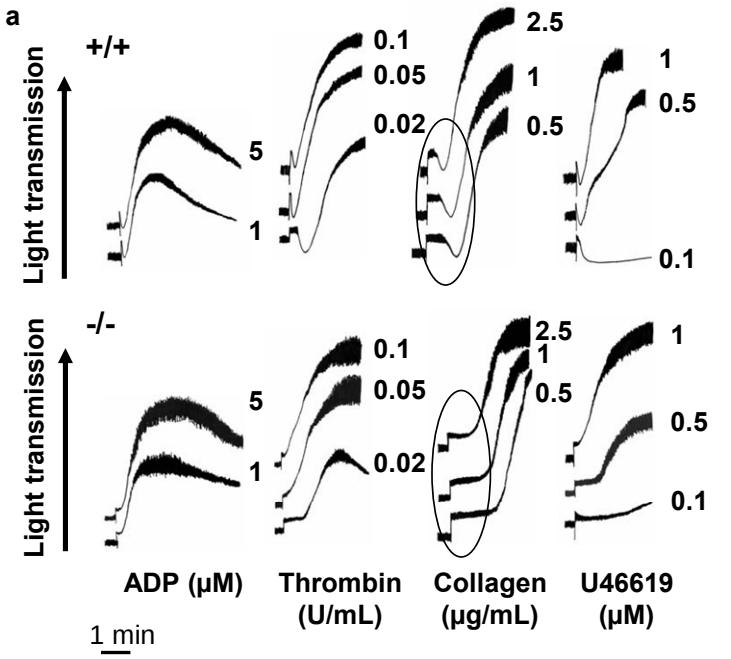
HAL author manuscript inserm-00166437, version 1

Figure 3



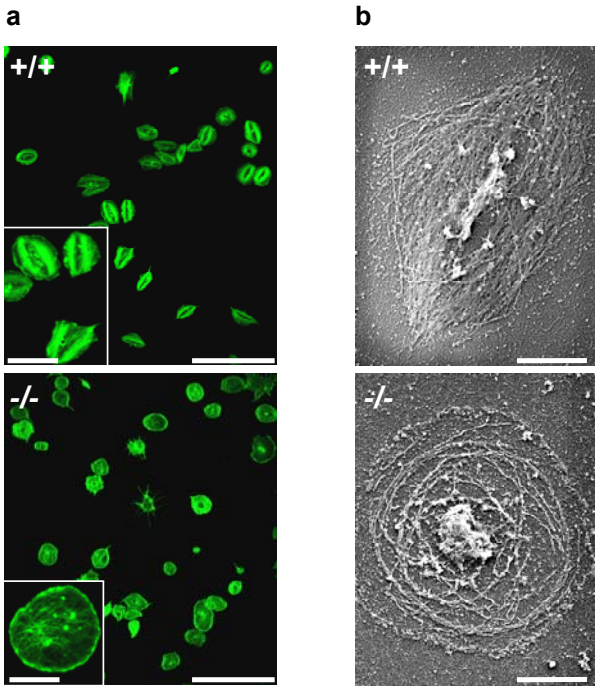
HAL author manuscript inserm-00166437, version 1

Figure 4



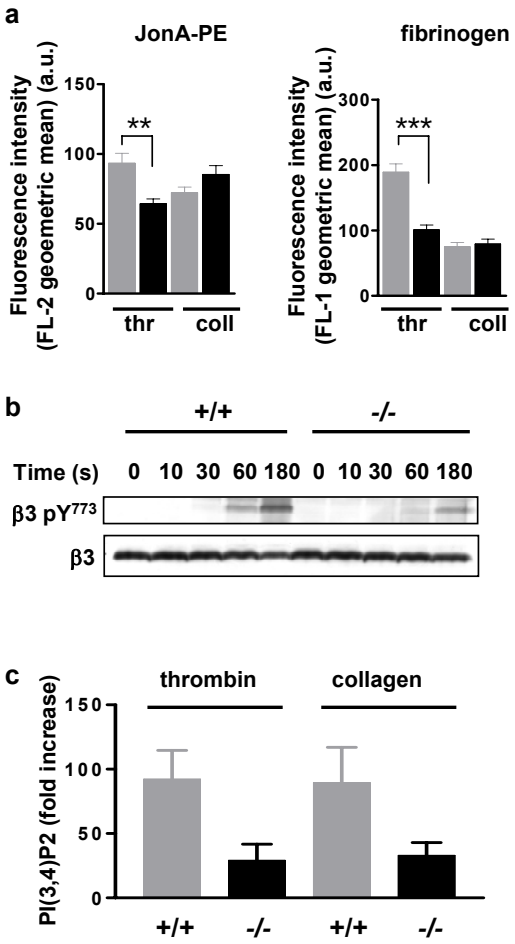
HAL author manuscript inserm-00166437, version 1

Figure 5



HAL author manuscript inserm-00166437, version 1

Figure 6



HAL author manuscript inserm-00166437, version 1

Figure 7

